Channel Estimation Method Using Power Control Schemes in Wireless Systems

Byounggi Kim and Sangjin Ryoo

Abstract: **Green communication is a new paradigm of designing the communication system which considers not only the processing performance but also the energy efficiency. Power control management is one of the approaches in green communication to reduce the power consumption in distributed communication system. In this paper, we propose improved power control schemes for mobile satellite systems with ancillary terrestrial components (ATCs). In order to increase system capacity and reduce the transmitting power of the user's equipment, we propose an efficient channel estimation method consisting of a modified open-loop power control (OLPC) and closed-loop power control (CLPC). The OLPC works well if the forward and reverse links are perfectly correlated. The CLPC is sensitive to round-trip delay and, therefore, it is not effective in a mobile satellite system. In order to solve the above problem, we added monitoring equipment to both the OLPC and CLPC to use information about transmitting power that has not yet been received by the receiver over the satellite/ATC channel. Moreover, we adapted an efficient pilot diversity of both OLPC and CLPC in order to get a better signal to interference plus noise ratio estimation of the received signal.**

Index Terms: **Channel estimation, power control.**

I. INTRODUCTION

Wireless communication has witnessed a continuous trend toward application diversification, leading to a significant growth in usage and services. With the proliferation of nomadic devices and multimedia applications, user demand is progressively shifting from simple data-rate increase to complex and heterogeneous quality of service (QoS) requirements. With these devices being powered, the performance requirements are coupled with severe constraints on energy efficiency. This is becoming a key concern. Thus, with the constant increase of power cost and awareness of global warming, the green communication concept has been introduced to improve an efficiency of communication resource usage. The concept of green radio is to develop environmental friendly, low-power and energy efficient solutions for future wireless networks. The objective of the green radio research is to deliver reduced power consumption of radio access networks. Power control is one of the major approaches in green communication to minimize the power consumption while the processing performance can be maintained at the target level. This power control can be implemented by controlling the operation mode of the communication resources.

Future systems should be able to fulfill the stringent requirements for QoS, mainly in terms of throughput, power efficiency, and error rate in green communication area. In 4G systems, the major role of satellites will be to provide terrestrial fill-in service and efficient multicasting/broadcasting services [1], [2]. However, it is known that it is difficult for a mobile satellite service (MSS) to reliably serve densely populated areas, because satellite signals are blocked by high-rise structures and/or do not penetrate into buildings. As a result, the satellite spectrum is significantly underutilized or unutilized in such areas. Under these circumstances, in a groundbreaking application to the Federal Communication Commission (FCC) in 2001, mobile satellite ventures LP (MSV) unveiled a bold new architecture for an MSS with an ancillary terrestrial component (ATC) providing unparalleled coverage and spectral efficiency [3]. The main concept of the hybrid MSS/ATC architecture of the MSV proposal is that terrestrial reuse of at least some of the satellite band service link frequencies can eliminate the above-mentioned problem [4]. As the terrestrial fill-in services using ATC, satellite systems provide services and applications similar to those of terrestrial systems outside the terrestrial coverage area as much as possible. In the future ubiquitous communication age, all the networks and services may be integrated [5], implying that keeping commonalities of technologies between networks is very important. In this regard, it is very important to keep commonalities between terrestrial networks. In addition, satellite systems, which have an advantage over terrestrial services for delivery of the same content to users spread over a wide geographic area, will effectively provide communication services, such as multimedia broadcast/multicast service (MBMS) [6].

Up to now, MSV has actively pursued study of MSS networks containing a global system for mobile (GSM)-based ATC systems compared with a code division multiple access (CDMA)-based ATC system. However, European satellite-universal mobile telecommunications systems (S-UMTS) along with terrestrial-universal mobile telecommunications systems (T-UMTS), whose standardization is underway at the European Telecommunications Standards Institute (ETSI), has adopted a WCDMA-based multiple access technology characterized as an asynchronous mode between cells [7]. Power control is one of the important issues in a CDMA system, because it has a significant impact on both performance and capacity. In addition, handover schemes between ATC and MSS are also a significant problem due to potential interference. This paper examines power control and handover using position information in land mobile satellite communication systems containing an ATC. In the power control of conventional land mobile satellite communication systems containing an ATC [8], the power control

Manuscript received October 28, 2009.

B. Kim is a Member of Research Staff at Huneed Technologies, 1-40 Hanrim Human Tower Geumjeong-dong, Gunpo-si, Gyeonggi-do, 435-824, Korea, email: kimbg@huneed.com.

S. Ryoo is corresponding author and is with the Department of Computer Media, Hanyeong College, San 19 Yeoseo-dong, Yeosu, Chonnam, 550-704, Korea, email: sjryoo@hanyeong.ac.kr.

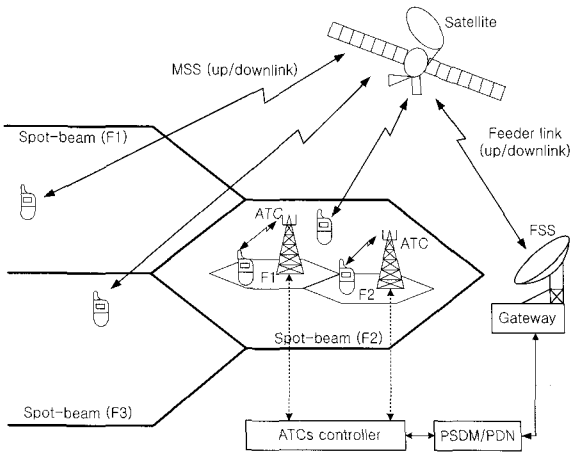

Fig. 1. MSV's hybrid system architecture.

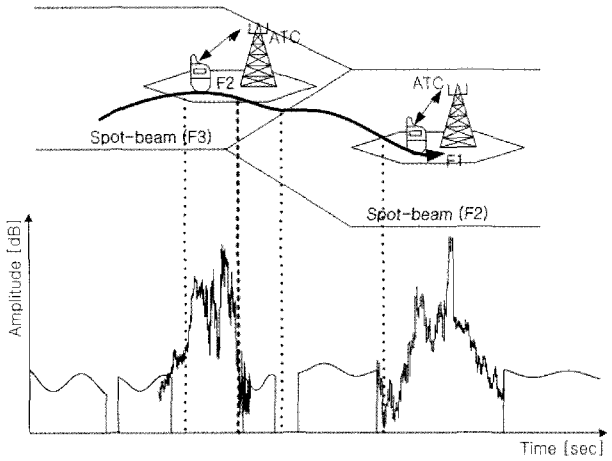

Fig. 2. Typical signal strengths received at multi-mode UE.

scheme of the user's equipment from the serving ATC is based on a combination of terrestrial open-loop and/or closed-loop methods, and the power control scheme of the user's equipment from the serving satellite is not described in detail.

However, in contrast to terrestrial communication systems, open-loop power control (OLPC) and closed-loop power control (CLPC) of land mobile satellite systems has only marginal benefit because of the lengthy round-trip delay (RTD) between the mobile unit and satellite (SAT)/ATC [9], [10]. In order to solve this problem, we consider adding monitoring equipment to use information about the transmitting power that has not yet experienced by the receiver over the SAT/ATC channel [11], [12]. In the handover part of conventional land mobile satellite communication systems containing an ATC, wireless communications with the user's equipment are handed over from the ATC to the satellite if the user's equipment transmitting power exceeds a threshold, an aggregate user's equipment interference exceeds a limit, and the received satellite signal quality exceeds a threshold, even if the user's equipment is able to wirelessly communicate with the ATC. However, modified handover methods can easily reduce the power of the user's equipment and increase system capacity by applying the proper maximum/minimum transmitting power to the corresponding system coverage (satellite or ATC) owing to the positioning information of the user's equipment. Moreover, if the user's equipment is edged from the predetermined distance from the serving ATC or the spot-beam of the satellite, the proposed algorithms perform an efficient handover using received diversity after receiving both spot-beams of the satellite and ATC. Based on these technological trends and requirements, we are currently developing efficient power control and handover technologies for a hybrid MSS/ATC system.

II. SYSTEM MODEL

Fig. 1 illustrates the MSV's hybrid system architecture. Land mobile satellite systems and methods are widely used in radiotelephone communications. The satellite is configured to transmit wireless communications to a plurality of users' equipment (UE), while the UE in a satellite footprint is composed of one or more satellite spot-beams over one or more MSS forward/reverse links [8]. The satellite is configured to receive wireless communications from, for example, UE in the satellite spot-beam over an MSS return link. An ATC network, composed of at least one ATC, which may include an antenna, is configured to receive wireless communications from other UE. ATC networks can enhance cellular satellite radiotelephone system availability, efficiency, and/or economic viability by terrestrially reusing at least some of the frequency bands that are allocated to cellular satellite radiotelephone systems.

In particular, it is known that it may be difficult for cellular satellite radiotelephone systems to reliably serve densely populated areas, because the satellite signal may be blocked by high-rise structures and/or may not penetrate into buildings [13]. As a result, the satellite spectrum may be underutilized or unutilized in such areas. The terrestrial reuse of at least some of a satellite band's frequencies can reduce or eliminate this potential problem. However, both accurate power control and efficient handover are vital, because all CDMA signals interfere with one another [14]. Lack of accurate power control reduces the capacity for CDMA. Moreover, power control can reduce battery drain and increase possible talk time [15]. The major objective of power control is to alleviate co-channel and cross-channel interference. For example, along the UE path, typical signal strengths from an ATC and a satellite in a multi-mode traveling from the ATC service coverage area to the satellite coverage area are shown in Fig. 2.

The ATC signal may decay more rapidly, as a function of distance away from a serving ATC, than the satellite signal owing to the high building density of the ATC environment [8]. The decay may not be monotonic owing to multi-path and shadowing effects. The satellite signal may have a combination of Rician fading and blockage. The UE may be configured to periodically monitor the signal qualities of itself and the satellite, which are potential candidates for a service handover from the ATC. In addition, the UE must perform power control if there is a serving ATC or satellite in order to reduce transmitting power and increase system capacity.

There are two types of power control: OLPC and CLPC. In CLPC, the reverse link (from UE to SAT/ATC) channel state is estimated by the SAT/ATC, then the base station issues a power

control command on the forward link (from SAT/ATC to UE) based on the estimation. In OLPC, the channel state on the forward link is estimated by the UE, and this information is used by the mobile unit as a measure of the channel state on the reverse link. OLPC works well if the forward and reverse links are perfectly correlated. The CLPC is sensitive to RTD and, therefore, it is not effective in a land mobile satellite system. In order to solve the above problem, we added monitoring equipment to both the OLPC and CLPC to use information about transmitting power that has not yet been received by the receiver over the SAT/ATC channel. Moreover, we adapted an efficient pilot diversity of both OLPC and CLPC in order to get a better signal to interference plus noise ratio (SIR) estimation of the received signal.

III. CHANNEL ESTIMATION

SIR estimation is one of the key aspects of the OLPC and CLPC scheme. SIR estimates are typically needed for functions such as power control, handoff, adaptive coding, and modulation. In this section, we focus on the third generation WCDMA FDD system and study the channel estimation in order to archive accurate energy of the desired signal [16], [17].

In wireless networks, signal fading arising from multi-path propagation is a particularly severe channel impairment that can be mitigated through the use of diversity, which amounts to transmitting the same information over multiple channels that fade independently of each other. Some popular diversity techniques are time diversity and frequency diversity, where the same information is transmitted at different time instants or in different frequency bands. Another technique is antenna diversity, in which one exploits the fact that fading is independent between different points in space [18]. We will focus on the pilot diversity technique, which is similar to time diversity.

The channel estimation using the pilot symbol structure periodically performs time-division multiplexing for data symbols and pilot symbols, which are known to a transmitter and a receiver, and transmits the multiplexed symbols. A channel change in a data symbol period is compensated with a channel estimation value in a pilot symbol period. The above channel estimation method is for estimating a channel using only the pilot symbols of a dedicated physical control channel (DPCCH). Another method compensates the data symbols for channel change by transferring pilot symbols, which are known to a transmitter and a receiver, using predetermined pilot symbol patterns. The above method estimates a channel using only a common pilot channel (CPICH). A disadvantage of the conventional channel estimation method is that it incurs more errors when a channel related to the channel estimation is under deep fading. It is, therefore, one of the objectives of our work to provide a channel estimation method with superior performance than channel estimation in a receiver of a terminal having conventional pilot symbols of a CPICH or a DPCCH. To this end, our method involves combining pilot symbols of a CPICH, a DPCCH, and a secondary common control physical channel (S-CCPCH), and estimating a channel.

Fig. 3 shows a relative timing correlation of the channel estimation method that combines the CPICH, DPCCH, and the S-CCPCH for the channel estimation in accordance with this paper. Efficient channel estimation is compared with a channel estimation method using only the pilot symbols of the CPICH, as well as a channel estimation method combining the pilot symbols of the DPCCH and those of the CPICH.

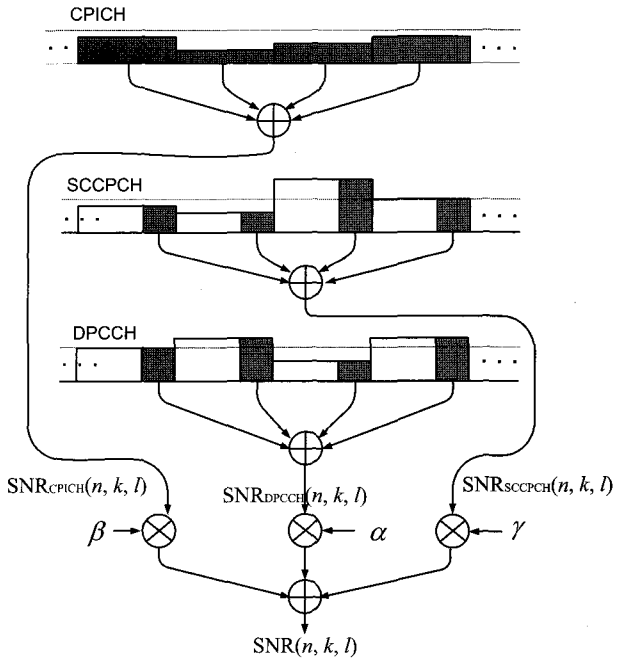

Fig. 3. A relative timing correlation of the channel estimation method that combines the CPICH/DPCCH/S-CCPCH.

A channel estimation using N symbols of the CPICH in one slot after a dispreading process in a RAKE receiver is represented as follows:

$$x(i) = \alpha(i) + n(i) \quad \text{for} \quad i = 1, 2, \cdots, N \tag{1}$$

in which N and $\alpha(i)$ are the number of pilot symbols in one slot of the CPICH and a channel gain to be estimated, respectively, and $n(i)$ is noise including the interference of other cells, which assumes zero mean and σ_n^2 variance. Equation (2) shows a method for estimating a channel by combining the pilot symbols of the DPCCH and CPICH. A receiver of a terminal acknowledges a pilot pattern for pilot symbols of the DPCCH in a manner similar to (1).

$$y(j) = \lambda(j)\alpha(j) + m(j) \quad \text{for} \quad j = 1, 2, \cdots, M \tag{2}$$

in which M is the number of pilot symbols in one slot of the DPCCH used in estimating a channel gain, and $\lambda(j) = (1/\mu(j))^{1/2}$ refers to the power ratio of the pilot symbols of the DPCCH and those of the CPICH. It is presumed that $m(j)$ is an additive white Gaussian noise (AWGN) that has zero mean and σ_m^2 variance. Since it is presumed that the channel gain is not changed during one slot of an estimation period, $\alpha(i)$ and $\lambda(i)$ become α and λ, respectively. Equation (3) shows a method for estimating a channel by combining the pilot symbols of the DPCCH, those of the CPICH, and those of the S-CCPCH.

$$z(k) = \lambda_1(k)\alpha(k) + l(k) \quad \text{for} \quad k = 1, 2, \cdots, K \tag{3}$$

in which K is the number of pilot symbols in one slot of the S-CCPCH used in estimating a channel gain, and $\lambda_1(k) = (1/\mu_1(k))^{1/2}$ refers to the power ratio of the pilot symbols of the S-CCPCH and those of the CPICH. It is presumed that $l(k)$ is an AWGN that has zero mean and σ_k^2 variance. Since it is presumed that the channel gain is not changed during one slot of an estimation period, $\alpha(k)$ and $\lambda_1(k)$ become α and λ_1, respectively. Since channelization codes used in the CPICH, the DPCCH, and the S-CCPCH are different from each other, $n(i)$, $m(j)$, and $l(k)$ are independent of each other. It is possible to perform the above processes, although the channels overlap at the same time. A vector of a signal received in a rake receiver of a terminal is as follows:

$$z' = [x(1)x(2)\cdots x(N)y(1)y(2)\cdots y(M)z(1)z(2)\cdots z(K)]^T \tag{4}$$

where T denotes an operator of a transpose matrix, α denotes a channel estimation value (case 1) using the CPICH, λ denotes a channel estimation value (case 2) combining the DPCCH and the CPICH [19], [20], and λ_1 denotes a channel estimation value (case 3) combining the CPICH, the DPCCH, and the S-CCPCH. A Cramer-Rao lower bound (CRLB) is used to analyze the performances of the above cases to compare channel estimation values of the above cases [21]. Then, a performance analysis is performed, as follows, by comparing case 2 with case 3 through the use of a Fisher information matrix. Subsequently, case 2 is compared with case 3, as described in (5), by using the aforementioned CRLB, to show that the performance of the developed method is superior to those of the other methods through the use of the Fisher information matrix [22].

$$\begin{aligned} I(\lambda_1,\alpha) &= \begin{bmatrix} -E\left(\frac{\partial^2 \ln p(z|\lambda_1,\lambda,\alpha)}{\partial^2\lambda_1}\right) & -E\left(\frac{\partial^2 \ln p(z|\lambda_1,\lambda,\alpha)}{\partial\lambda_1\partial\alpha}\right) \\ -E\left(\frac{\partial^2 \ln p(z|\lambda_1,\lambda,\alpha)}{\partial\alpha\partial\lambda_1}\right) & -E\left(\frac{\partial^2 \ln p(z|\lambda_1,\lambda,\alpha)}{\partial^2\alpha}\right) \end{bmatrix} \\ &= \begin{bmatrix} \frac{K\lambda^2\alpha^2}{\sigma_k^2} & \frac{2\lambda_1\lambda^2\alpha K}{\sigma_k^2} \\ \frac{2\lambda_1\lambda^2\alpha K}{\sigma_k^2}\frac{N}{\sigma_n^2} + \frac{M\lambda^2}{\sigma_m^2} + \frac{K\lambda_1^2\lambda^2}{\sigma_k^2} & \end{bmatrix} \end{aligned} \tag{5}$$

If λ_1 is known, the output CRLB is as follows [18]:

$$\begin{aligned} \mathrm{CRLB}(\hat{a} \mid \lambda_1) &= \frac{1}{I(\lambda_1,\alpha)_{2,2}} \\ &= \frac{1}{\frac{N}{\sigma_n^2} + \frac{M}{\mu\sigma_m^2} + \frac{K}{\mu\mu_1\sigma_k^2}} \le \frac{1}{\frac{N}{\sigma_n^2} + \frac{M\lambda^2}{\sigma_m^2}} \le \frac{\sigma_n^2}{N} \end{aligned} \tag{6}$$

As a result, it can be seen that the channel estimation combining the CPICH, the DPCCH, and the S-CCPCH is superior to both the channel estimation using only the CPICH and the channel estimation combining the CPICH and the DPCCH.

IV. OPEN-LOOP POWER CONTROL

Conventionally, uplink and downlink power control may be based on a combination of open- and/or closed-loop methods. A modified OLPC and CLPC model is shown in Fig. 4. In the OLPC, the UE estimates a transmitting power level, which may maintain a desired signal quality and/or strength at a base transceiver system (BTS) or base station, by monitoring its

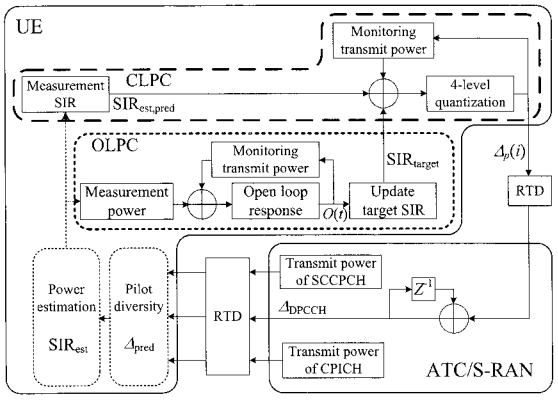

Fig. 4. Modified OLPC and CLPC model.

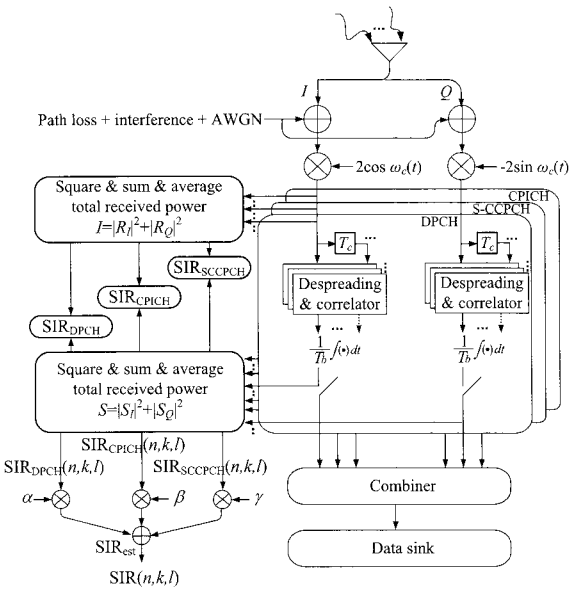

Fig. 5. Block diagram of power estimation using pilot diversity.

own received quality. In other words, the mobile's transmitting power is determined by measuring the received signal strength of the base station and estimating the forward link path loss. Assuming a similar path loss for the reverse link, the mobile unit uses this information to determine its transmitter power. In the IS-95 system reverse link, power control is used to compensate for the signal power fluctuation at the base station due to path loss and shadowing, as well as small-scale fading. This technique is crucial to the system performance, due to its role in preventing a near-far effect and in mitigating fading. The OLPC adjusts the transmitted signal power level according to the received forward link signal strength. Hence, it mainly compensates for path loss and shadowing, while the CLPC is designed to compensate for the small-scale fading caused by the multipath in the transmission on the reverse link, which is different from that on the forward link, due to the frequency separation of the links. As mentioned in Section III, in order to improve the accuracy of the estimation of SIR, we proposed a method to estimate the interference power, which will be presented as follows.

In Fig. 5, n, k, l, T_b, and T_c denote nth slot, kth symbol, lth resoluble multi-path, bit duration, and chip duration, respectively. In addition, $\mathrm{SIR}_{\mathrm{DPCH}}(n,k,l)$, $\mathrm{SIR}_{\mathrm{CPICH}}(n,k,l)$, and $\mathrm{SIR}_{\mathrm{SCCPCH}}(n,k,l)$ stand for estimates of the dedicated physical channel (DPCH), CPICH, and S-CCPCH, respectively. SIR is an important power control system parameter that has a profound effect on system capacity as the desired signal and the interference have the same bandwidth at the output of the digitally matched filter, SIR. Since the interference noise is Gaussian distributed, the variance of the interference can be found from the sum of the variances of the amplitude of the I channel and Q channel, as follows [23]:

$$I = E\left|R_I\right|^2 + E\left|R_Q\right|^2 \tag{7}$$

The inphase and quadrature components of the received signal, namely I and Q, corrupted by interference noise become R_I and R_Q, respectively. Desired signal S is achieved by calculating the summation of the S_l from the 1 to L tap RAKE receiver.

$$S = \sum_{l=0}^{L-1} S_l \tag{8}$$

According to Friis' free-space propagation-path-loss formula [24], in order to apply OLPC, the average received power at the mobile unit would be

$$P_r = |E|^2 / 2\eta_0 = P_0[1/(4\pi d/\lambda)]^2 \tag{9}$$

where $P_0 = P_t G_t G_m$, η_0 is the intrinsic impedance of free-space, P_t is the transmitted power, G_t is the gain of the transmitting antenna, and G_m is the gain of the receiving antenna.

Path loss and shadowing effects are regarded as slow fading in this work. To compensate for slow fading, the CDMA 2000 system has defined a standard equation for the mobile station to perform OLPC for the air interface in [25]. The general open-loop response of the OLPC can be approximated as follows [26]:

$$O(t) = -\Delta P_{\mathrm{in}}(1 - \exp(-t/\tau)u(t). \tag{10}$$

In (10), ΔP_{in}, τ, and $O(t)$ are the step change in mean input power, the time constant of the open-loop response, and the output. The OLPC output response of UE serving from ATC is close to that specified in the standards if τ is 20 ms. We assume that the operation period of the OLPC output response of UE serving from a geostationary earth orbit (GEO) satellite is 250 ms. In this paper, it is added to the monitoring equipment in OLPC to use information about the transmitting power that has not yet been received by the receiver over the SAT/ATC channel.

V. CLOSED-LOOP POWER CONTROL

CLPC is a powerful tool to mitigate near-far problems in a direct-sequence code division multiple access (DS-CDMA) system over Rayleigh fading channels [27]. The SAT/ATC advises the UE of adjustments to the transmitting power level that may have initially been set by the OLPC. This form of power control (open- and/or closed-loop) may increase the UE's effective isotropically radiated power (EIRP) to the maximum in order to maintain link connectivity and/or acceptable link quality. Because of a significant difference in the RTD, there is serious performance degradation of the CLPC if the power control used for the terrestrial interface is employed as is. In order to reduce power control error, a delay compensation mechanism was selected in the ATC and satellite.

For the case of the uplink CLPC, the UE calculates the actual amount of the transmission power control by using the two most recently received power control commands, which are aimed to change the loop dynamics and shorten the latency in updating the transmission power. For the case of the downlink CLPC, the UE may employ a prediction algorithm that estimates the future SIR value after an RTD by observing the SIR of the CPICH and S-CCPCH. The power control command is generated on the basis of the predicted SIR value. The RTD of a GEO system results in significant performance degradation of the CLPC if the 3GPP standard is employed as is [28]. There are two main problems that degrade the CLPC under such a long RTD. The first problem is instability in the internal loop dynamics, because the power control step size specified in 3GPP is too large to keep the loop stable under such a long loop delay. In other words, the measurements at the UE do not reflect the results of the most recent power updates at the satellite radio access network (S-RAN) and ATC network. The second problem is the possibility of a large number of SIR changes during the loop delay, resulting in a large power control error. As an effective solution to the first problem, Gunnarsson proposed a delay compensation power control scheme [11], [12], and this was reflected in the S-UMTS standard [29]. Although this can effectively cancel the internal RTD in the power control loop, the second problem remains.

In order to solve the second problem, we proposed a prediction algorithm that estimates the future SIR value after an RTD. We now present our proposed algorithm in more detail by focusing on the downlink CLPC scheme. We apply it to a GEO system, and will demonstrate delay compensation performance. The power control adjusts the SAT/ATC radio access network (S-RAN) transmitting power in order to keep the received downlink power SIR at a given SIR target, $\mathrm{SIR}_{\mathrm{target}}$. The UE estimates the SIR of the received downlink DPCCH and the SIR variation of the received CPICH and S-CCPCH, where the CPICH channel and the S-CCPCH are not power controlled and are power controlled, respectively, then generates two-bit transmitting power control (TPC) commands every 10 ms (per frame) [30]. The TPC commands are generated as follows. Firstly, let us define power control error of $\Delta_{\varepsilon,c} = \mathrm{SIR}_{\mathrm{est}} - \mathrm{SIR}_{\mathrm{target}} + \Delta_{\mathrm{loop\ delay}}$, where $\Delta_{\mathrm{loop\ delay}}$ and $\mathrm{SIR}_{\mathrm{est}}$ denote the prediction for the amount of SIR increment/decrement of the received downlink CPICH, S-CCPCH, and the estimated SIR of the received downlink DPCCH during the next time interval equal to the loop delay, respectively. Therefore, $\Delta_{\mathrm{loop\ delay}}$ is added to $\mathrm{SIR}_{\mathrm{est}}$ to result in the predicted SIR value of $\mathrm{SIR}_{\mathrm{est,pred}}$. In other words, we employed a simple algorithm to calculate $\Delta_{\mathrm{loop\ delay}}$ as follows:

$$\Delta_{\mathrm{loop\ delay}} = n\Delta_{\mathrm{pred}} \tag{11}$$

where $n\Delta_{\mathrm{pred}}$ is the increment (or decrement) of the estimated SIR of CPICH and S-CCPCH in dB during the last frame, and n

Table 1. Simulation environment.

Parameter	Value	
Carrier frequency (f_c)	2,170 MHz	
Power control sample interval (T_d)	UE serving from GEO satellite	10 ms
	UE serving from ATC	6.667E - 4 ms
Frame length	10 ms	
Round trip delay	GEO satellite	250 ms
	ATC	< slot duration (≈ 6.667E - 4 ms)
Processing gain	256 (≈ 24 dB)	
Transmit frame	UE serving from GEO satellite	70,000 frames
	UE serving from ATC	60,000 slots
Small step size	1 dB	
Large step size	2 dB	
Fading model	Clarke's model (Classical Doppler spectrum)	
Target SIR	5 dB	
Desired received power	- 140 dBW (≅ - 110 dBm)	
Rician K-factor	UE serving from GEO satellite	5 dB
	UE serving from ATC	- inf
Power command error probability	0 ~ 0.15	
Interference plus noise power	- 123 dBm	
Interference variance	6 dB	
Path loss variance	8 dB	
Maximum transmitting power	GEO satellite	41.8 dBW
	ATC	28 dBm
Minimum transmitting power	GEO satellite	- 2.9 dBW
	ATC	- 61 dBm
Mobile speed	0 ~ 98 km/h	

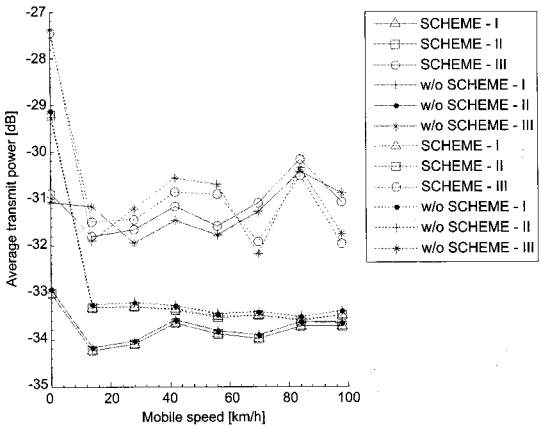

Fig. 6. Average transmitting power of UE from ATC according to mobile speed.

is the nearest integer to (loop delay)/(frame length). A four-level quantized power control step, Δ_p, is generated according to the region of Δ, as follows:

If $|\Delta_{\varepsilon,c}| < \varepsilon_T$ and $\Delta_{\varepsilon,c} < 0$, $\Delta_p(i) = \Delta_S$.
If $|\Delta_{\varepsilon,c}| < \varepsilon_T$ and $\Delta_{\varepsilon,c} > 0$, $\Delta_p(i) = -\Delta_S$.
If $|\Delta_{\varepsilon,c}| > \varepsilon_T$ and $\Delta_{\varepsilon,c} < 0$, $\Delta_p(i) = \Delta_L$.
If $|\Delta_{\varepsilon,c}| > \varepsilon_T$ and $\Delta_{\varepsilon,c} > 0$, $\Delta_p(i) = -\Delta_L$.

In the statements above, Δ_S, Δ_L, and ε_T are a small power control step, a large power control step, and the error threshold, respectively. Because of the RTD in the GEO system, the S-RAN can reflect $\Delta_p(i)$ at its transmission power after about 250 ms, during which time there may be a considerable change in the SIR. We employ a simple preprocessing for $\Delta_p(i)$ before it is reflected at the transmission power in order to compensate for the RTD. The S-RAN adjusts the transmitting power of the downlink DPCCH with an amount of DPCCH using the two most recently received power control steps, $\Delta_p(i)$ and $\Delta_p(i-1)$, and this can be modeled as a simple finite impulse response filter (FIR), as follows [31]:

$$\begin{aligned}\Delta_{\mathrm{DPCCH}} &= \Delta_p(i) - \alpha\Delta_p(i-1) \\ &= (1-\alpha)\Delta_p(i) + \alpha(\Delta_p(i) - \Delta_p(i-1)) \end{aligned} \quad (12)$$

which means that Δ_{DPCCH} is determined not only by $\Delta_p(i)$ but also by the difference between $\Delta_p(i)$ and $\Delta_p(i-1)$ with weighting factors of $(1-\alpha)$ and α, respectively. As α increases, Δ_{DPCCH} becomes more dependent upon the term $\Delta_p(i) - \Delta_p(i-1)$, which corresponds to an estimate for the amount of the recent channel variation.

VI. SIMULATION RESULTS

A channel with only fast fading and a channel with path loss, slow fading, and fast fading were simulated to examine the performance of the CLPC with and without an OLPC. The simulation parameters are given in Table 1. We present the simulation results of only the proposed CLPC scheme (SCHEME-II), combining the proposed OLPC and proposed CLPC (SCHEME-I), and only the proposed OLPC (SCHEME-III) over GEO satellite

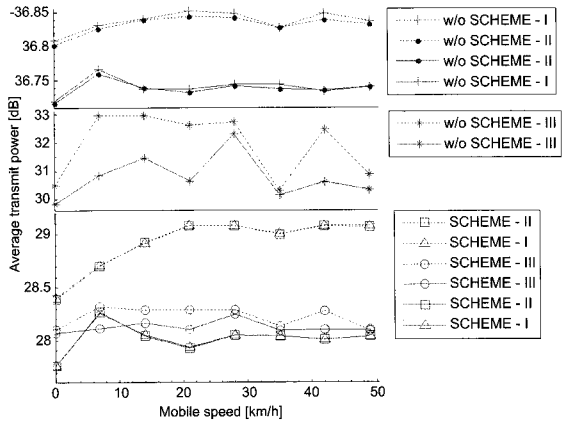

Fig. 7. Average transmitting power of UE from GEO satellite according to mobile speed.

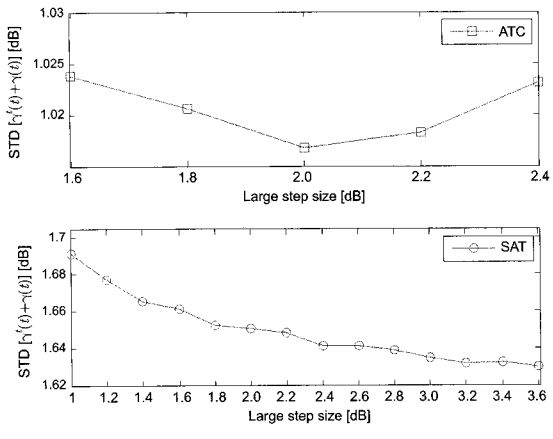

Fig. 8. Power control error versus large power control step size.

or ATC environments, and we compare the performance of the various conventional- OLPC and CLPC algorithms [11], [26]. For conventional schemes, we used the terrestrial CLPC scheme

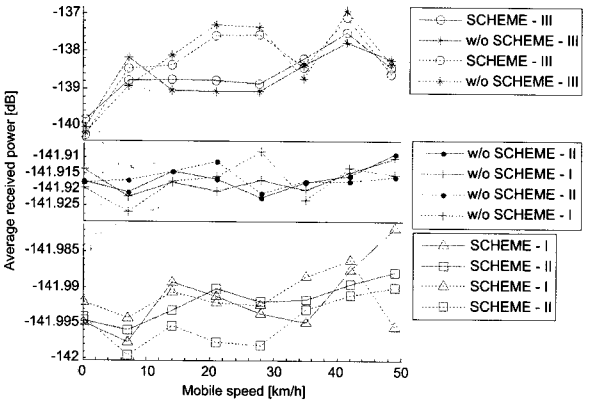

Fig. 9. Received average power of UE from ATC according to mobile speed.

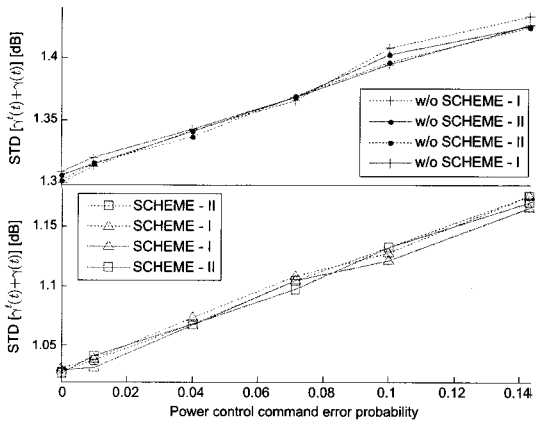

Fig. 11. Control error of UE serving from ATC: Standard deviation of target SIR minus received SIR with increased power control command error probability.

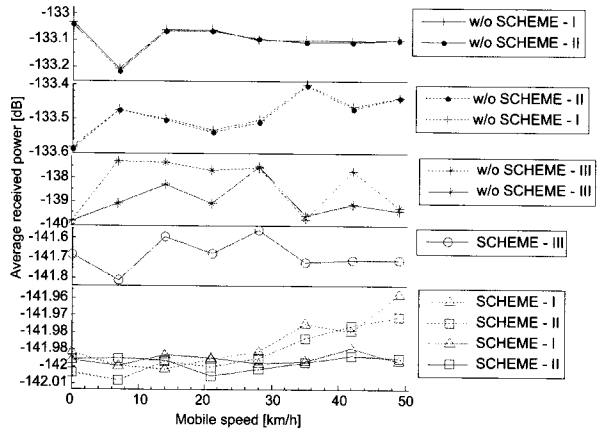

Fig. 10. Received average power of UE from GEO satellite according to mobile speed.

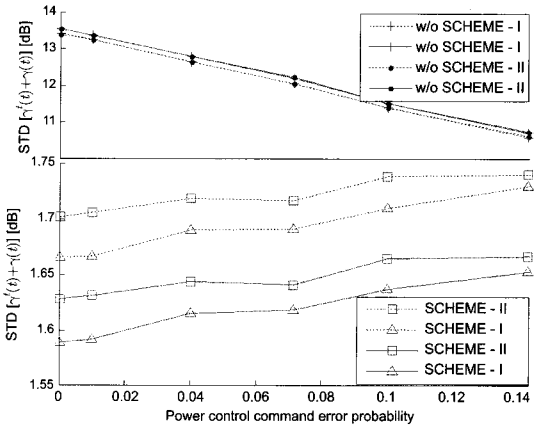

Fig. 12. Control error of UE serving from GEO satellite: Standard deviation of target SIR minus received SIR with increased power control command error probability.

in the WCDMA system [26] and Gunnarsson's scheme in [11], and they are denoted in the figures as SCHEME-II with a dotted line and without SCHEME-II with a dotted line. For reference, the part shown as the dotted line and solid line means without pilot diversity and with pilot diversity, respectively. In our simulations, we consider a satellite system with a single beam and ignore the inter-spot interference. We assume that the path loss exponent is taken to be 2. For the simulations, we chose a target SIR of 5 dB. We selected a processing gain (PG) of 256. We assumed power control begins to work after 250 ms due to propagation delay.

Figs. 6 and 7 show the average transmitting power consumed at the transmitters of specific users according to mobile speed. It is observed that average UE transmitted power of all schemes is dependent of mobile speed. However, we can see that users with a combination of the modified OLPC and CLPC scheme consume less power. It is also seen that at low vehicle speeds (< 40 km/h), combining modified OLPC and CLPC (SCHEME-I shown with a solid line) is very effective. This is because SCHEME-I compensates slow fading and path loss by monitoring transmitting power of UE and simultaneously archives diversity gain by using efficient channel estimation algorithms. Assuming the same parameters for the channel and a mobile velocity of 56 km/h, Fig. 8 shows the standard deviation between the target SIR and the received SIR, according to different large power control step sizes when a small power control step size is fixed at 1 dB. First, for the UE served by the ATC, if a step size is too small, it may not be efficient to compensate for the channel fading; on the other hand, if the step size is too large, it may overly compensate and thus introduce extra variance in power control error. The optimal step size in this example is about 2 dB. Second, it is known that power control errors can be reduced by using a high, large power control step size, because a power control error is dependent on path loss and the shadowing effect compared with channel gain for the UE served by ATC. Therefore, to keep commonalities between terrestrial networks, small and large step sizes of 1 and 2 dB, respectively, were used.

Figs. 9 and 10 show the average received power consumed at the transmitters of specific users according to mobile speed. We

can see that the received power of users with a combination of the modified OLPC and CLPC scheme using pilot diversity is settled compared to the other scheme. This highlights the importance of monitoring transmitting power equipment applying for a CDMA-based system. With a RAKE receiver, the dynamic range of the received power decreased as the monitoring equipment decreased.

Figs. 11 and 12 describe control error in the case of a mobile velocity of 56 km/s, showing the probability of power control command error from 0 to 0.15, respectively. As seen in the simulation results, the conventional power control methods incur many errors in the case of deep fading. On the other hand, since the proposed power control using the S-CCPCH to the conventional channel estimation methods can achieve an improved pilot diversity gain by performing the channel estimation using another channel in case the first channel does not reach a required level of a received signal, it is possible to implement an ideal maximum ratio combination method in a RAKE receiver. The lower power consumption will also directly lead to capacity increase. The superior power control performance is due to the more efficient estimation of SIR.

Assuming the same parameters for the channel and a mobile speed of 98 km/h, performance of our system and the other system with increased power control command error probability is illustrated in Figs. 13 and 14. As shown in the figures, the combined proposed OLPC and CLPC (SCHEME-I shown in solid line) is also still powerful compared to other system. This algorithm efficiently removes the shadowing effect and simultaneous slow/fast fading of the UE serving from the GEO satellite. For the UE serving from ATC, the power control error of SCHEME-I using pilot diversity is superior to the other scheme when the normalized Doppler frequency of the UE is zero because of power estimation when using pilot diversity. However, it is seen that at low vehicle speeds (14 ~ 42 km/h), performance of SCHEME-I and II which is monitoring transmitting power is inferior to other schemes because conventional CLPC is an insensitive short RTD. We note in Fig. 13 that the standard deviations in the power control error of SCHEME-I with pilot diversity, SCHEME-II with pilot diversity, SCHEME-I without pilot diversity, and SCHEME-II without pilot diversity were 1.0156 dB, 1.0157 dB, 1.024 dB, and 1.023 dB, respectively, when mobile speed was 70 km/h. There was a decrease in the standard deviation of errors in SIR for the scheme with the pilot diversity compared with the other scheme. We also observed that the increase in the standard deviation due to combining monitoring transmitting power and the OLPC scheme became relatively smaller as the mobile speed increased from 0 km/h to 96 km/h. Figs. 13 and 14 illustrate power control error according to mobile speed. When employing our efficient pilot diversity and monitoring equipment of power control scheme, power control shows greater stability, which is important in the sense of the network. From Figs. 13 and 14, we observe that the standard deviation of the power control error in SIR increased as the mobile speed increased. In Fig. 14, for SCHEME-I using pilot diversity, the standard deviation of the power control error in SIR was 1.59 dB for a mobile speed of 56 km/h, while that in SCHEME-II using pilot diversity was approximately 1.65 dB for a mobile speed of 56 km/h. The combining of monitoring

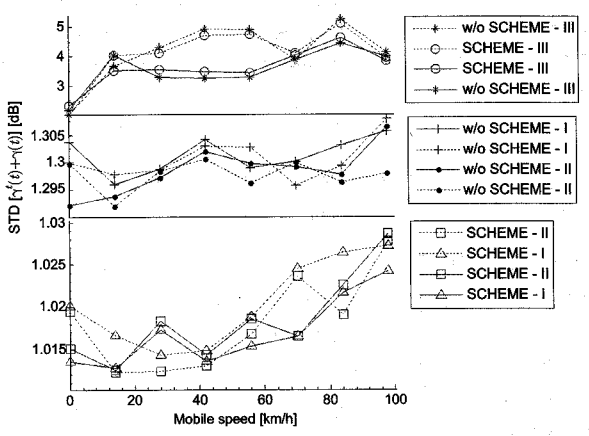

Fig. 13. Control error UE serving from ATC: Standard deviation of target SIR minus received SIR according to mobile speed.

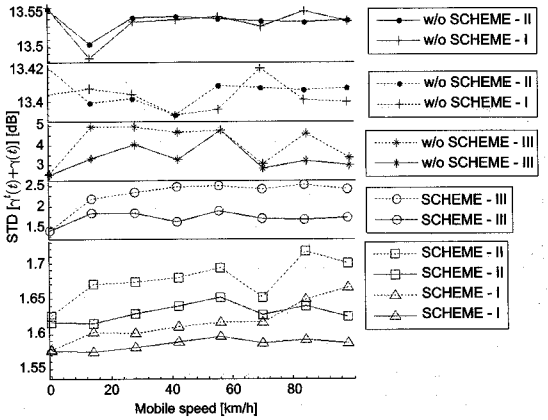

Fig. 14. Control error UE serving from GEO satellite: Standard deviation of target SIR minus received SIR according to mobile speed.

transmitting power and OLPC scheme in SCHEME-I using pilot diversity efficiently removed path loss and slow fading, because if fast fading can be approximately tracked, then there is little difficulty in coping with much slower variations in path loss and slow fading.

Figs. 15 and 16 show the probability density function of the received SIRs for a mobile speed of 98 km/h having a probability of power control command error of 0. Intuitively, we turn out that the SCHEME-I using pilot diversity has a larger improvement, as confirmed in the simulation results. Fig. 17 shows the received SIRs of the UE when it is handed over from the GEO satellite to the ATC. As we can see, the powers of the user in the case described in Fig. 16 with SCHEME-I using pilot diversity converge to the target SIR of 5 dB. On the other hand, those of the other schemes result in a higher SIR estimation error.

VII. CONCLUSION

Conventional channel estimation methods incur many errors in the case of deep fading. In contrast, the proposed channel estimation method using the S-CCPCH to the conventional methods

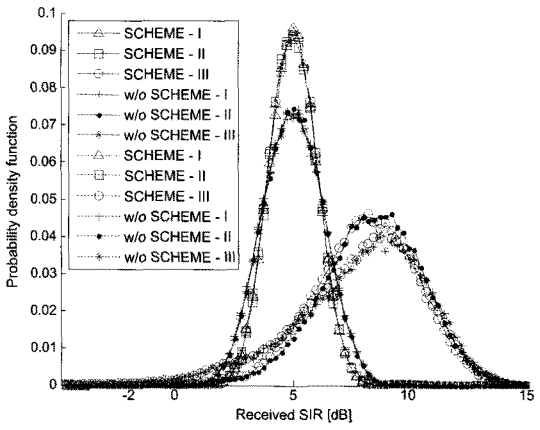

Fig. 15. Histogram of received SIRs of UE serving from ATC: $K = -\infty$ and $V = 98$ km/h.

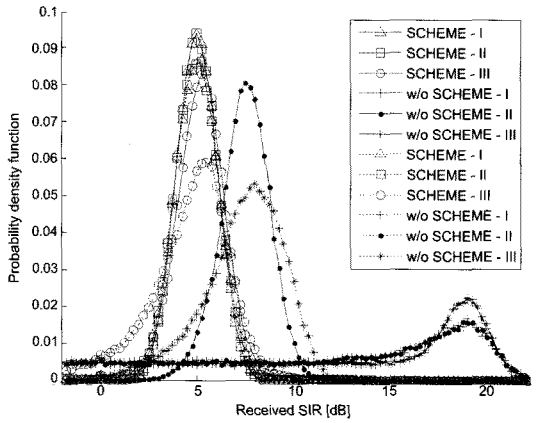

Fig. 16. Histogram of received SIRs of UE serving from GEO satellite: $K = 5$ dB and $V = 98$ km/h.

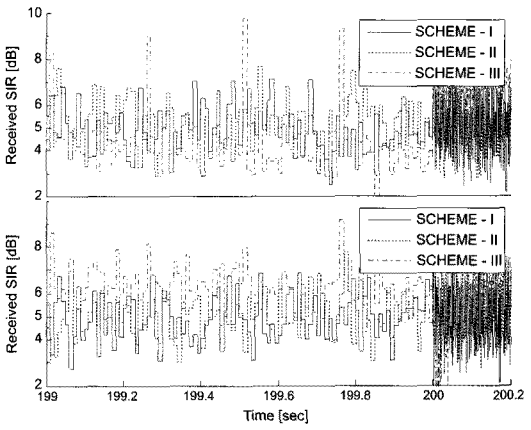

Fig. 17. Received SIRs of UE when is handed over from the GEO satellite to ATC: $K = 5$ dB, $V = 14$ km/h (up: Without pilot diversity, bottom: With pilot diversity.)

can obtain an improved pilot diversity gain by performing channel estimation using other channels when the first channel does not reach a required level of a received signal. Thus, it is possible to implement an ideal maximum ratio combining method in a RAKE receiver. The channel estimation method described in this paper provides a more improved performance than channel estimation in a receiver of a terminal having conventional pilot symbols of a CPICH or a DPCCH by combining pilot symbols of a CPICH, a DPCCH, and a S-CCPCH, and estimating a channel. Simulation results show that the proposed channel estimation method has good performance compared to conventional channel estimation method in a GEO satellite system utilizing ATCs.

In this paper, we have presented satellite access technologies for a future mobile system. We suggested desirable modifications for application to the 4G system. Combining modified CLPC and OLPC with delay compensation algorithms and monitoring equipment proved to provide a good performance in a MSS/ATC hybrid system. In addition, to increase the performance and to keep commonalities between terrestrial standards, more advanced transmission technologies, including multi-carrier transmission, interference cancelation, and highly efficient modulation and coding should be investigated in more detail. As a result, green (or environmentally friendly) communication systems will emerge, which offer a wide variety and ubiquitous availability of wireless services, while overcoming energy and spectrum scarcity.

REFERENCES

[1] "Estimates of MSS subscriber numbers and traffic profiles for the ASMS-TF," ESYS Consulting, 2003.

[2] I. Philipopoulos, S. Panagiotarakis, and A. Yanelli-Coralli, "The role of S-UMTS in future 3G markets," *IST-2000-25030 SATIN Project*, SUMTS.P-specific requirement, deliverable No. 2, Apr. 2002.

[3] G. M. Parson and R. Singh, "An ATC primer: The future of communications," MSV. 2006.

[4] "Flexibility for delivery of communications by mobile satellite service providers in the 2 Ghz band, the L-band, and the 1.6/2.4 bands," IB, Report and Order and Notice of Proposed Rulemaking, FCC 03-15, Adopted: Jan. 29, 2003, Released: Feb., 10. 2003.

[5] P. Conforto, C. Tocci, G. Losquadro, R. E. Sheriff, P. M. L. Chan, and Y. Fun Hu, "Ubiquitous Internet in an integrated satellite-terrestrial environment: The SUITED solution," *IEEE Commun. Mag.*, vol. 40, pp. 98–107, Jan. 2002.

[6] "Introduction of the multimedia broadcast multicast service (MBMS) in the radio access network (RAN)," Third Generation Partnership Project (3GPP) Technical Specification 25-346, Stage 2, Release 6, Mar. 2004.

[7] "Satellite earth stations and systems (SES); satellite component of UMTS/IMT-2000; evaluation of the W-CDMA UTRA FDD as a satellite radio interface," ETSI TR 102 058, Nov. 2004.

[8] S. Dutta and D. Karabinis, "Systems and methods for handover between space based and terrestrial radioterminal communications, and for monitoring terrestrially reused satellite frequencies at a radioterminal to reduce potential interference," US Patent no. 6879829 B2, Apr. 12, 2005.

[9] A. M. Monk and A. Chockalingam, L. B. Milstein, "Open-loop power control error on a frequency selective CDMA channel," in *Proc. IEEE GLOBECOM*, Dec. 1994, pp. 29–33.

[10] A. M. Monk and L. B. Milstein, "Open-loop power control error in a land mobile satellite system," *IEEE J. Sel. Areas Commun.*, vol. 13, no. 2, pp. 205–212, Feb. 1995.

[11] F. Gunnarsson, F. Gustafsson, and J. Blom, "Dynamical effects of time delays and time delay compensation in power controlled DS-CDMA," *IEEE J. Sel. Areas Commun.*, vol. 19, no. 1, pp. 141–151, Jan. 2001.

[12] F. Gunnarsson and F. Gustafsson, "Time delay compensation in power controlled cellular radio systems," *IEEE Commun. Lett.*, vol. 5, no. 7, pp. 295–297, July 2001.

[13] P. D. Karabinis, S. Dutta, and W. W. Chapman, "Interference potential to MSS due to terrestrial reuse of satellite band frequencies," in *Proc. ICSSC*, 2005.

[14] K. S. Gihousen, I. M. Jacobs, R. Padovani, A. J. Viterbi, L. A. Weaver, and C. E. Wheatley, "On the capacity of a cellular CDMA system," *IEEE Trans. Veh. Technol.*, vol. 40, no. 2, pp. 303–312, May 1991.
[15] J. S. Lehnert, "An efficient technique for evaluation direct-sequence spread-spectrum multiple access communications," *IEEE Trans. Comm.*, vol. 37, no. 8, pp. 851–858, Aug. 1989.
[16] D. Pauluzzi and N. Beaulieu, "A comparison of SNR estimation techniques for the AWGN channel," *IEEE Trans. Commun.*, vol. 48, no. 10, pp. 1681–1691, Oct. 2000.
[17] S. Seo, T. Dohi, and F. Adachi, "SIR-based transmit power control of reverse link for coherent DS-CDMA mobile radio," *IEICE Trans. Commun.*, vol. E81-B, no. 7, pp. 1508–1516, July 1998.
[18] H. V. Khuong and H. Y. Kong, "BER performance of cooperative transmission for the uplink of TDD-CDMA systems," *ETRI J.*, vol. 28, no. 1, pp. 17–30, Feb. 2006.
[19] T. Luo and Y. C. Ko, "Pilot diversity channel estimation in power-controlled CDMA systems," *IEEE Trans. Veh. Technol.*, vol. 53, no. 2, pp. 559–563, Mar. 2004.
[20] M. Usuda, Y. Ishikawa, and S. Onoe, "Optimizing the number fo dedicated pilot symbols for forward link in WCDMA systems," in *Proc. IEEE VTC*, June 2000, pp. 2118-2122.
[21] S. M. Kay, *Fundamentals of Statistical Signal Processing: Esimation Theory, 2nd ed.* Englewood Cliffs, NJ: Prentice-Hall, 1993.
[22] R. Zamir, "A proof of the Fisher information matrix inequality via a data processing argument," *IEEE Trans. Inf. Theory*, vol. 44, pp. 1246–1250, 1998.
[23] C.-C. Lee and R. Steele, "Closed-loop power control in CDMA systems," *IEE Proc. Commun.*, vol, 143, no. 4, pp. 231–239, Aug. 1996.
[24] C. William and Y. Lee, *Mobile Communications Engineering, 2nd ed.*, McGraw-Hill, 1998.
[25] "Physical layer standard for cdma2000 spread spectrum systems-Release 0," 3GPP2 TSG-C, May 2001.
[26] S. Choe, "An analytical framework for imperfect DS-CDMA closed-loop power control over flat fading," *ETRI J.*, vol. 27, no. 6, pp. 810–813, Dec. 2005.
[27] T. Chulajata and H. M. Kwon, "Combinations of power controls for cdma2000 wireless communications system," in *Proc. IEEE VTC*, vol. 2, Sept. 2000, pp. 638–645.
[28] "Physical layer-procedures (FDD)—Release 5," 3GPP TS 25.214, 2004.
[29] "Satellite component of UMTS/IMT2000: A-family: Part 4, physical layer procedures (S-UMTS-A 25.214)," ETSI TS 101 851-4, Nov. 2000.
[30] "Detailed specifications of radio interfaces of IMT-2000," Recommendation ITU-R M.1457, 2001.
[31] K. Lim, K. Choi, K. Kang, S. Kim, and H. J. Lee, "A satellite radio interface for IMT-2000," *ETRI J.*, vol, 24, no. 6, pp. 415–428, Dec. 2002.

Byounggi Kim received his B.S. and M.S. degrees in computer engineering from Chonnam National University, Korea, in 2001 and 2003. From 2004 to 2008 he was employed at Broadband Wireless Technology Group of ETRI, Korea. He is currently a Member of Research Staff at the Huneed Technologies, and has worked for the development of efficient transmission algorithms for military communications. His research interests include satellite communications, military communications, and multicarrier transmission.

Sangjin Ryoo received the B.S., M.S., and Ph.D. degrees in electronics engineering from Chonnam National University, Korea, in 1991, 1994, and 2007, respectively. Since March 1994, he has been with the Department of Computer Media, Hanyeong College, Yeosu, Korea. His research areas are BS/MS modem design, communication theory, signal processing, and advanced channel codes for wireless communication systems. He is currently interested in Mobile Telecommunication and satellite communications, IMIT-Advanced communication systems, channel coding, AMC, MIMO, and MIMO-OFDM systems.